A possible explanation of the knee of cosmic light component spectrum from 100 TeV to 3 PeV*

Wen-Hui Lin(林文慧) Bi-Wen Bao(鲍必文) Ze-Jun Jiang(姜泽军)[1] Li Zhang(张力)[2]

Department of Astronomy, Yunnan University, Key Laboratory of Astroparticle physics of Yunnan Province, Kunming 650091, China

Abstract: A mixed hydrogen and helium (H + He) spectrum with a clear steepening at ~ 700 TeV has been detected by the ARGO-YBJ experiments. In this paper, we demonstrate that the observed H + He spectrum can be reproduced well with a model of cosmic rays escaping from the supernova remnants (SNRs) in our Galaxy. In this model, particles are accelerated in a SNR through a non-linear diffusive shock acceleration mechanism. Three components of high energy light nuclei escaped from the SNR are considered. It should be noted that the proton spectrum observed by KASCADE can be also explained by this model given a higher acceleration efficiency.

Keywords: cosmic Rays, particle acceleration, supernova remnants, amplified magnetic field

PACS: 98.38.Mz, 98.58.Db, 95.85.Pw **DOI:** 10.1088/1674-1137/41/10/105101

1 Introduction

Supernova remnants (SNRs) are generally believed to be the origin of Galactic cosmic rays (CRs) [1–5]. The explanation of the knee at $\sim 3\times10^{15}$ eV as a feature coinciding with the maximum energy of the light component of cosmic rays and the transition to a gradually heavier mass composition is mainly based on KASCADE results [6]. Some recent data, however, appear to challenge this finding: the combined detection of showers with a wide field of view Cherenkov telescope (WFCT) and ARGO-YBJ find a flux reduction in the light component at $\sim$ 700 TeV [7], a factor $\sim$0.2 of the previous result. This observed result favors the origin of SNRs in our Galaxy and helps us understand the acceleration mechanism inside the SNRs.

Diffusive shock acceleration (DSA) is assumed to take place inside a SNR as an efficient particle acceleration mechanism [8–11]. However, a high acceleration efficiency implies strong coupling between the accelerated particle population, the shock structure, and the electromagnetic fluctuations, resulting in a non-linear diffusive shock acceleration (NLDSA) [6, 12, 13]. To solve the NLDSA problem, three approaches have been proposed: kinetic semi-analytic solutions, Monte Carlo numerical simulations of the full particle population, and fully numerical simulations. The results obtained with the three different techniques are consistent with each other in terms of both accelerated spectra and hydrodynamics (see a review in Ref. [14]). We will base our analysis on the kinetic semi-analytical model given by Ref. [15], for its computational convenience.

In this paper, we will investigate the properties of particle spectra efficiently accelerated in Galactic SNRs and try to provide a possible explanation of the position of the knee of the light component cosmic ray spectrum observed by ARGO-YBJ [7] and KASCADE [16–18]. The paper is structured as follows. We give a brief review of the NLDSA model of Ref. [15] in Section 2, and apply this model to explain the observed light component cosmic ray spectra in Section 3. A summary is given in Section 4.

2 Review of NLDSA model

In the NLDSA model given by Ref. [15], the shock is placed at a distance $x=0$, so the upstream and downstream region correspond to $x<0$ and $x>0$, respectively. Physical quantities measured at upstream infinity, immediately upstream of the shock, and downstream are labelled by subscripts 0, 1, and 2, respectively. Generally, it is convenient to define two different compression ratios for subshock and total shock [19]: $r_{\rm sub}=\tilde{u}_1/\tilde{u}_2$ and $r_{\rm tot}=\tilde{u}_0/\tilde{u}_2$, where $\tilde{u}=u+u_{\rm A}$, u is the bulk plasma velocity in the shock frame, and $u_{\rm A}$ is the Alfvén velocity with respect to the background plasma.

In such a system, a diffusive-convection equation describing the transport of the ith particles in the shock

Received 4 May 2017, Revised 3 July 2017

∗ Supported by the National Natural Science Foundation of China (11433004, 11363006, 11103016, 11173020), Top Talents Program of Yunnan Province (2015HA030) and the Natural Science Foundation of Yunnan Province(2015FB103)

1) E-mail: zjjiang@ynu.edu.cn

2) E-mail: lizhang@ynu.edu.cn

frame can be expressed as [15]:

$$\tilde{u}\frac{\partial f_i}{\partial x}=\frac{p}{3}\frac{\partial\tilde{u}}{\partial x}\frac{\partial f_i}{\partial p}+\frac{\partial}{\partial x}\left[\kappa_i(x,p)\frac{\partial f_i}{\partial x}\right]+Q_i(x,p), \quad (1)$$

where subscript i represents the ith particles, $f_i=f_i(x,p)$ is the distribution function of the ith particles, and $\kappa_i(x,p)$ is the Bohm-like parallel diffusion coefficient with a magnetic field strength $B(x)$ and is given by

$$\kappa_i(x,p)=\frac{u(x)}{3}r_{\rm L}(x,p)=\frac{u(x)pc}{3Z_ieB(x)}, \quad (2)$$

$Q_i(x,p)$ is the ith particle injection term and is given by

$$Q_i(x,p)=\eta_i\frac{n_0u_0}{4\pi p_{{\rm inj},i}^2}\delta(p-p_{{\rm inj},i})\delta(x), \quad (3)$$

where η_i is the fraction of the ith particles crossing the shock injected in the acceleration process, $p_{{\rm inj},i}=Z_i\,p_{\rm inj,H}$ is the injection momentum of the ith particles, and $\delta(x)$ is the position where particles are injected at the shock. In the thermal-leakage model [15, 20],

$$p_{\rm inj,H}=\xi_{\rm H}\sqrt{2m_{\rm H}k_{\rm B}T_{\rm H,2}}, \quad (4)$$

$$T_{\rm H,2}=T_0(R_{\rm tot}/R_{\rm sub})^{\gamma-1}\frac{\gamma+1-(\gamma-1)R_{\rm sub}^{-1}}{\gamma+1-(\gamma-1)R_{\rm sub}}, \quad (5)$$

where $k_{\rm B}$ is the Boltzmann constant, $m_{\rm H}$ is the proton mass, γ=5/3 is the ratio of specific heats of gas and $\xi_{\rm H}$ is a parameter which defines $p_{\rm inj,H}$ as a part of the momentum of the thermal protons in the downstream region.

In the absence of the dynamical back-reaction of the accelerated particles and magnetic field amplification at the shock, Eq. (1) can be independently solved. In other words, the pressure of the accelerated particles $P_{\rm CR}(x)$ and magnetic field pressure $P_{\rm B}(x)$ are negligible in comparison with the pressure $P_{\rm g}(x)$ of the gas with a density ρ. In this case (called the test particle approximation), the conservation equations of mass, momentum and energy across the shock have the trivial solutions: ρ= constant, u= constant, and $P_{\rm g}$= constant.

In a general case, the two non-linear effects above must be considered.

(1) the dynamical back-reaction of the accelerated particles. Because the particles are efficiently accelerated at the shock, the pressure $P_{\rm CR}$ of the accelerated particles must be included in the energy conservation equation, which results in a slowing down of upstream plasma velocity in the shock frame, forming a so-called dynamical shock precursor. The normalized pressure of the accelerated particles can be estimated as

$$P_{\rm CR}(x)=\frac{4\pi}{3\rho_0u_0^2}\sum_i\int_{p_{{\rm inj},i}}^{\infty}{\rm d}pp^3\tilde{u}(x)f_i(x,p). \quad (6)$$

(2) the effect of the magnetic field amplification. Here, magnetic field amplification due to the streaming instability of plasma flow is considered. In this case, the streaming instability of plasma flow will lead to magnetic field amplification, and then the magnetic pressure ($P_{\rm B}$) will change significantly and affect shock compression ratios and particle spectra. Following Ref. [15], the normalized pressure of the magnetic field can be expressed as

$$P_{\rm B}(x)=\frac{2}{25}\frac{[1-U(x)^{5/4}]^2}{U(x)^{3/2}}, \quad (7)$$

where $U(x)=(\rho/\rho_0)[u^2(x)/u_0^2]$. The amplified magnetic field is then estimated as

$$B(x)=\sqrt{8\pi P_{\rm B}(x)}. \quad (8)$$

Considering both of the effects mentioned above, the momentum conservation equation, normalized to $\rho_0u_0^2$, can be represented as:

$$U(x)+P_{\rm CR}(x)+P_{\rm B}(x)+P_{\rm g}(x)=1+\frac{1}{\gamma M_0^2}, \quad (9)$$

where $P_{\rm CR}(x)$ and $P_{\rm B}(x)$ are given by Eqs. (6) and (7), respectively, $P_{\rm g}(x)=\frac{U(x)^{-\gamma}}{\gamma M_0^2}$ is the normalized pressure of the background gas with adiabatic index γ, and $M_0=\frac{u_0}{c_s}$ is the Mach number of the fluid at upstream infinity.

Equation (1) with the spatial boundary condition $f_i(x_0,p)=0$ has been solved and the solution can be expressed as [19]

$$f_i(x,p)=f_{{\rm sh},i}(p){\rm e}^{-\int_x^0{\rm d}x'\frac{\tilde{u}(x')}{\kappa_i(x',p)}\left[1-\frac{W_i(x,p)}{W_{i,0}(p)}\right]}, \quad (10)$$

where $f_{{\rm sh},i}(p)$ is the distribution function at the shock, and is

$$f_{{\rm sh},i}(p)=\frac{\eta_in_0q_{{\rm p},i}(p)}{4\pi p_{{\rm inj},i}^3}{\rm e}^{\left\{-\int_{p_{{\rm inj},i}}^p\frac{{\rm d}p'}{p'}q_{{\rm p},i}(p')\left[U_{{\rm p},i}(p')+\frac{1}{W_{i,0}(p')}\right]\right\}}, \quad (11)$$

where $U_{{\rm p},i}(p)=U_1-\int_{x_0}^0{\rm d}x[{\rm d}U(x)/{\rm d}x][f_i(x,p)/f_{{\rm sh},i}(p)]$ and $q_{{\rm p},i}(p)=3R_{\rm tot}/(R_{\rm tot}U_{{\rm p},i}(p)-1)$; the function $W_i(x,p)$ in Eq. (10) is given by

$$W_i(x,p)=\int_x^0{\rm d}x'\frac{u_0}{\kappa_i(x',p)}{\rm e}^{\int_{x'}^0{\rm d}x''\frac{\tilde{u}(x'')}{\kappa_i(x'',p)}} \quad (12)$$

and $W_{i,0}(p)=W_i(p)|_{x=x_0}$. The escape flux can be written as

$$\Phi_{{\rm esc},i}(p)=-\kappa_i(x,p)\left.\frac{\partial f_i}{\partial x}\right|_{x_0}=-\frac{u_0f_{{\rm sh},i}(p)}{W_{i,0}(p)}. \quad (13)$$

Therefore, Eq. (1) is coupled with the equations describing mass, momentum, and energy flux conservations, leading to the NLDSA problem whose solution can be obtained through the iterative method described in Refs. [19] and [21].

3 Particle injection from a SNR

To perform our calculation, the following assumptions about a SNR's evolution are made: the SNR is pro-

duced in a supernova explosion with an energy $E_{\rm SN}=10^{51}$ erg and an ejecta mass $M_{\rm ej}=1.4M_{\odot}$, and a shock moves with velocity $u_0=4000$ km/s in a homogeneous and hot medium with a number density $n_0=0.01$ cm^{-3}, a temperature $T_0=10^6$ K and a background magnetic field $B_0=5$ μG. According to the analytical recipe given in Ref. [22], the SNR evolution is divided into two stages [15]:

(1) Ejecta-dominated stage with $\tau=t/T_{\rm ST}\leqslant 1$, where the radius and velocity of the SNR are given by

$$R_{\rm sh}(t)\simeq 14.1\tau^{4/7}\ {\rm pc}, \tag{14}$$

$$V_{\rm sh}(t)\simeq 4140\tau^{-3/7}\ {\rm km/s}, \tag{15}$$

where $T_{\rm ST}\simeq 2000$ a is used;

(2) Sedov - Taylor stage with $\tau=t/T_{\rm ST}\geqslant 1$,

$$R_{\rm sh}(t)\simeq 16.2(\tau-0.3)^{2/5}\ {\rm pc}, \tag{16}$$

$$V_{\rm sh}(t)\simeq 3330(\tau-0.3)^{-3/5}\ {\rm km/s}. \tag{17}$$

Adiabatic loss is included because of the shell expansion. The energy $E(t)$ of a particle with energy E_0 advected downstream at time t_0 is given by Ref. [15] where $4/3\leqslant\gamma\leqslant 5/3$.

The accelerated particles can escape from a shell volume $V=4\pi R_{\rm sh}^2{\rm d}R_{\rm sh}$, where ${\rm d}R_{\rm sh}=V_2(t){\rm d}t=[V_{\rm sh}(t)/r_{\rm tot}]{\rm d}t$ and ${\rm d}t$ is the time increment. Since the particle number per unit volume per unit energy can be expressed as $J_i(E,t)=4\pi p^2 f_{{\rm sh},i}(p){\rm d}p/{\rm d}E$, where $f_{{\rm sh},i}(p)$ is the distribution function at shock radius $R_{\rm sh}(t)$, the particle number per unit energy in the shell volume V can be estimated as $J_i(E,t)\times V$. Because the shell volume evolves with time t during SNR evolution, the particle number per unit energy is

$$\phi_i(E)=4\pi\int_{T_{\rm ini}}^{T_{\rm fin}}J_i(E,t)R_{\rm sh}^2(t)[V_{\rm sh}(t)/r_{\rm tot}]{\rm d}t, \tag{18}$$

where $T_{\rm ini}$ and $T_{\rm fin}$ are the initial and final times of the SNR evolution. Here, $T_{\rm ini}=0.1T_{\rm ST}$ and $T_{\rm fin}=15T_{\rm ST}$ with $T_{\rm ST}=2000$ a are used. There are three kinds of components for the particles escaping from the SNR [19]:

(1) The numbers per unit energy of particles which instantaneously escape around a maximum momentum $p_{\rm max}(t)$ from the upstream free escape boundary at $x=x_0$ during the Sedov - Taylor (ST) stage, where $p_{\rm max}(t)$ is determined by the finite size of the SNR during the ST stage, which can be estimated by $\kappa_i(p_{\rm max})/V_{\rm sh}(t)\approx\chi R_{\rm sh}(t)$, assuming x_0 to be a fraction χ of the radius $R_{\rm sh}(t)$ of the SNR with a shock velocity $V_{\rm sh}(t)$. In this case, the number density of particles per unit energy is $4\pi p^2(\Phi_{{\rm esc},i}(p)/V_{\rm sh}(t_0)){\rm d}p/{\rm d}E$, where $\Phi_{{\rm esc},i}(p)$ is given by Eq. (13), therefore the particle numbers per unit energy are

$$q_{{\rm esc},i}(E_0)=\frac{16\pi^2}{c^2}\int_{T_{\rm ini}}^{T_{\rm fin}}pR_{\rm sh}^2(t)E_0\frac{\Phi_{{\rm esc},i}(p)}{r_{\rm tot}}{\rm d}t. \tag{19}$$

(2) The numbers per unit energy of particles which are advected in the downstream region, leading to adiabatic loss as a consequence of the shell expansion, where the particles can escape at $p>p_{\rm esc}(t)$ at any given time and $p_{\rm esc}(t)$ can be estimated by $\kappa_i(p_{\rm esc},B_2)/V_2=x_0$ with $V_2=V_{\rm sh}/r_{\rm tot}$. In this case, the particle numbers per unit energy are

$$q_{{\rm adv},i}(E_0)=\frac{16\pi^2}{c^2}\int_{T_{\rm ini}}^{T_{\rm fin}}pR_{\rm sh}^2(t)E_0f_{{\rm sh},i}(p)\frac{V_{\rm sh}(t_0)}{r_{\rm tot}}\times\left(\frac{V_{\rm sh}(t)}{V_{\rm sh}(t_0)}\right)^{2/3\gamma}{\rm d}t. \tag{20}$$

(3) The numbers per unit energy of particles which escape the acceleration region from a broken shell at the end of a SNR's evolution,

$$q_{{\rm shell},i}(E_0)=\lambda\times\frac{16\pi^2}{c^2}\int_{T_{\rm ini}}^{T_{\rm fin}}pR_{\rm sh}^2(t)E_0f_{{\rm sh},i}(p)\frac{V_{\rm sh}(t_0)}{r_{\rm tot}}{\rm d}t, \tag{21}$$

where the fraction of downstream escaping particles is taken as $\lambda\approx 10\%$.

Therefore, the numbers per unit energy of the ith particles escaping from a single SNR is the sum of Eqs. (19) – (21), i. e.,

$$q_i(E)=q_{{\rm esc},i}(E)+q_{{\rm adv},i}(E)+q_{{\rm shell},i}(E). \tag{22}$$

As an example, the spectra of H and He nuclei injected into interstellar space are shown in Fig. 1. The model parameters are as follows: $\xi_{\rm H}=3.0$, $\chi=0.5$ $T_0=10^6$ K, $n_0=0.01$ cm^{-3}, and $B_0=5$ μG. In this figure, the spectra of three components mentioned above for H and

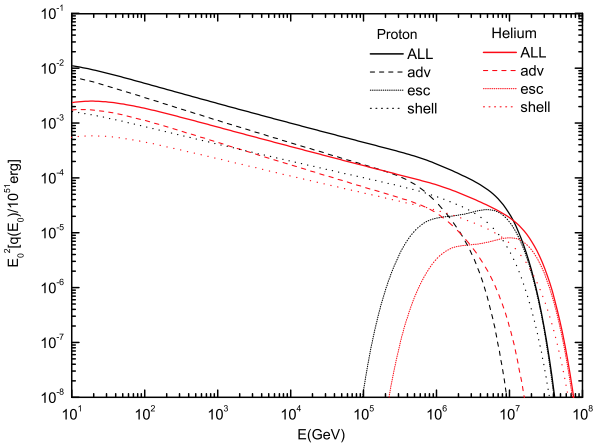

Fig. 1. (color online) Escape spectra of protons and He nuclei from a single SNR. Three components of the escape spectra for protons (black line) and He (red line) nuclei are presented by long dashed, dotted, and short dashed lines. The black and red solid lines represent the total spectra of protons and He nuclei, respectively. The model parameters are $\xi_{\rm H}=3.0$, $\chi=0.5$, $T_0=10^6$ K, $n_0=0.01$ cm^{-3}, and $B_0=5$ μG.

He nuclei have been shown. From the figure, the first component dominates the high-energy end, and the second component is the main contributor at lower energy. Moreover, from the bell-shaped curves (dotted line), which show that the particles escaped from the upstream boundary of the SNR, we can see that escaping occurs at the highest energies. The cut-off energy of He is larger than that of H. For the parameters used here, the shock is modified by the accelerated particles: $r_{\rm sub}$=3.41 and $r_{\rm tot}$=4.73.

Note that one parameter has an important influence on the CR spectrum, the parameter $\xi_{\rm H}$, which describes the acceleration efficiency. In Fig. 2, it can be seen that the lower acceleration efficiency (i.e., a larger $\xi_{\rm H}$) of the particles, the flatter the resulting spectra and the smaller the maximum energy.

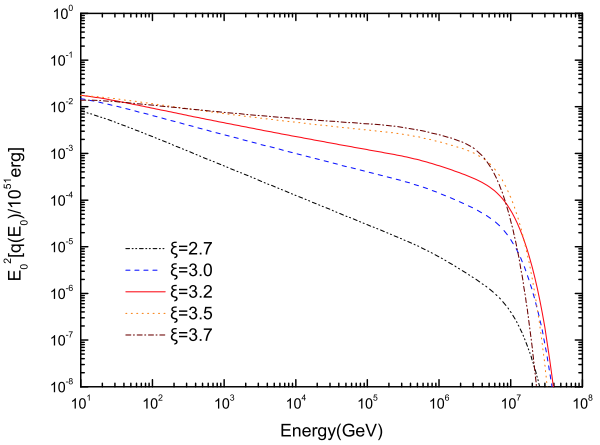

Fig. 2. (color online) Cumulative proton spectra for $\xi_{\rm H}$ = 2.7 (dash-dot-dotted line), $\xi_{\rm H}$ = 3.0 (dashed line), $\xi_{\rm H}$=3.2 (solid line), $\xi_{\rm H}$=3.5 (dotted line) and $\xi_{\rm H}$=3.7 (dash-dotted line).

4 Proton and He spectra observed at the earth

In this section, the spectra of H and He nuclei observed at the Earth are calculated. It is assumed that the propagation can be approximated by a simple leaky box model with a 3 percent SN explosion rate in our Galaxy. In this case, the energy spectrum $N_i(E)$ of the ith particles observed at the Earth is given by [23]

$$N_i(E)\propto q_i(E)\left(\frac{1}{\lambda_{{\rm esc},i}}+\frac{1}{\lambda_{{\rm int},i}}\right)^{-1}, \qquad (23)$$

where the escape path length $\lambda_{{\rm esc},i}$ is a function of the particle magnetic rigidity $R_i = pc/Z_i$ and is approximated as $\lambda_{\rm esc} = 7.3(R_i/10\ {\rm GV})^{-\delta}\beta(p)$ g/cm^2, where $\delta = 0.3-0.6$, $\beta(p)$ is the dimensionless speed of a nucleus of momentum p, $\lambda_{{\rm int},i}$ is the interaction length and $\lambda_{{\rm int},i}=\lambda_{0,i}(E/10\ {\rm GeV})^{-\epsilon_{\rm i}}$, where $\lambda_{0,{\rm H}}=\lambda_{0,{\rm He}}=50$ g cm^{-2}, $\epsilon_{\rm H}$=0.05, $\epsilon_{\rm He}$=0.0416 [23].

In order to estimate the value of η_i from the measurement, following Ref. [24], the ratio of abundances between ions and protons at the same momentum $p*=10^5$ GeV/c measured at the Earth is defined as $K_{i{\rm H}}=n_i/n_{\rm H}$, and $\eta_i/\eta_{\rm H}\approx K_{i{\rm H}}Z_i^{-(\delta+\beta-3)}$. The distribution function is assumed to be a power law with a slope β, which can be obtained in the test particle approximation. Here $\beta+\delta$=4.7 is used [24], so $\eta_{\rm He}/\eta_{\rm H}\approx 0.31K_{\rm He\ H}$.

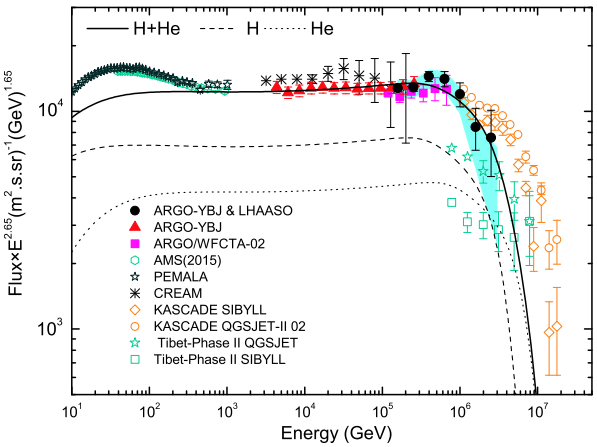

Fig. 3. (color online) Comparison of our model results with the observed H + He flux. The observed data are taken from ARGO-YBJ [7, 25, 26], AMS [27, 28], PAMELA [29], CREAM [30], the hybrid experiment [26] below the knee, Tibet AS$_\gamma$ [31], and KASCADE [16–18] above the knee. Long dashed and short dashed lines represent predicted fluxes of H and He components, respectively, and the solid line is the flux sum of two components. Model parameters are $\xi_{\rm H}$=3.8, δ=0.55, χ=0.5, $T_0=10^6$ K, n_0=0.01 cm^{-3}, and B_0=5 μG.

Figure 3 shows a comparison of our model results with the H + He flux observed by the ARGO-YBJ experiments [7, 25, 26]. The H + He spectrum has a knee feature of ∼700 TeV [7]. For comparison, the observed data from various experiment groups are also shown. It can be seen from the figure that our model results can reproduce the flux observed by the ARGO-YBJ experiments well. Moreover, the knee feature can be explained by the sum of H and He spectra but the He spectrum dominates the high energy end. Note that the acceleration is efficient in this case, $\xi_{\rm H}$=3.8 corresponds to $\eta_{\rm H}\approx 6.5\times10^{-5}$ and $\eta_{\rm He}\approx 0.31K_{\rm He\ H}\times\eta_{\rm H}\sim 2.01\times10^{-5}$. The deviation at low energy may be due to solar modulation, which we did not consider in our model.

As mentioned above, the acceleration efficiency plays an important role for the cut-off energy of the spectrum in the model. The KASCADE experiments [16] show that the observed H spectrum has a knee feature at a few PeV, which is not consistent with that observed by

the ARGO-YBJ experiment [7, 25, 26]. To reproduce the H flux observed by the KASCADE experiments with our model, the acceleration efficiency (i.e. $\xi_{\rm H}$) is properly adjusted but other parameters are not changed for the proton injection spectrum, and the comparison of the model result with the observed H flux is shown in Fig. 4. With $\xi_{\rm H}=3.5$ and $\delta=0.5$, the observed H flux can be reproduced well in this model.

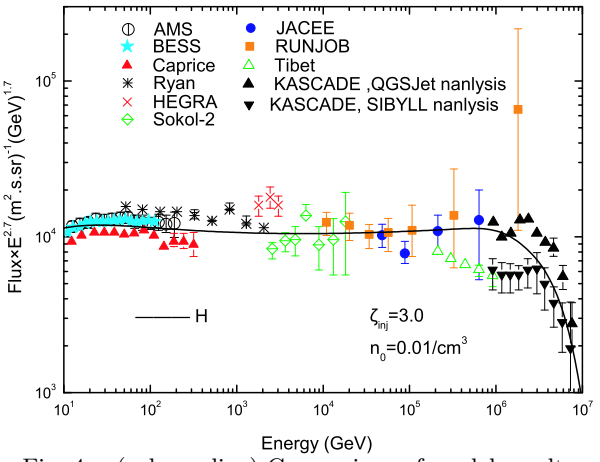

Fig. 4. (color online) Comparison of model results with observed H flux. The solid line is the H flux predicted in the model. Model parameters are $\xi_{\rm H}=3.5$, $\delta=0.5$, $\chi=0.5$, $T_0=10^6$ K, $n_0=0.01$ cm^{-3}, and B_0=5 μG.

5 Results and discussion

In this paper, the observed spectra of the light component (P+He) by the ARGO-YBJ and the proton spectrum by the KASCADE experiments are reproduced in the framework of the non-linear diffusive shock acceleration model of SNRs. In the model, the escape spectrum of ith particles injected into the ISM consists of three components (see Eqs. (19), (20) and (21)). In our calculation, for the case with ARGO-YBJ, parameter $\xi_{\rm H}=3.8$ is used, which corresponds to $\eta_{\rm H}\approx6.5\times10^{-5}$ and $\eta_{\rm He}\approx0.31K_{\rm He\ H}\times\eta_{\rm H}\sim2.01\times10^{-5}$, and $\eta_{\rm H}\approx4.32\times10^{-4}$ for the case with KASCADE. These values indicate that the acceleration at the SNR shock is very efficient. In fact, it is generally believed that the acceleration is inefficient when $\eta_{\rm H}<\sim10^{-5}$, which implies the acceleration efficiency is less than a few % [15].

Finally, it should be pointed out that a typical evolution scenario of SNRs in our Galaxy and a simple leaky box approximation of CR propagation are used in our calculations. In fact, the situation is very complicated [24] and the detailed processes of the CR spectrum reaching the knee through NLDSA remain uncertain. Meanwhile, the variations of parameters have a strong influence on the distribution of the knee. The contributions of different classes of SNRs to the CR spectrum should be taken into account [32] and a more relativistic CR propagation model [33] should be used. It can be predicted that data with smaller uncertainties will constrain the parameters (e.g the amplified magnetic field) and demonstrate the effectiveness of the model.

The authors would like to thank the anonymous referee for insightful comments. We also thank Prof. Xiaohui Sun for helpful discussions and suggestions.

References

1 W. Baade, F. Zwicky, Physical Review, **46**: 76–77 (1934)
2 V. A. Acciari, E. Aliu, T. Arlen et al, Astrophys. J., **730**: L20 (2011)
3 F. Giordano, M. Naumann-Godo, J. Ballet et al, Astrophys. J., **744**:L2 (2012)
4 J. Vink, Astron. Astrophys. Rev., **20**: 49 (2012)
5 M. Ackermann, M. Ajello, A. Allafort et al, Science, **339**: 807 (2013)
6 P. Blasi, Nuclear Physics B, **256**, 36 (2014)
7 B. Bartoli et al, Phys. Rev. D, **92**, 092005 (2015)
8 G. F. Krymskii, Akademiia Nauk SSSR Doklady, **234**: 1306–1308 (1977)
9 R. D. Blandford, J. P. Ostriker, Astrophys. J., **221**: L29–L32 (1978)
10 W. I. Axford, E. Leer, G. Skadron, Proc. 15th. Int. Cosmic. Ray. Conf., **11**: 132 (1977)
11 A. R. Bell, MON. Not. R. Astron. Soc., **182**: 147 (1978)
12 M. A. Malkov & L. Drury, Reports on Progress in Physics, **64**: 429 (2001)
13 A. M. Bykov, D. C. Ellison, S. M. Osipov et al, Astrophys. J, **789**: 137 (2014)
14 D. Caprioli, H. Kang, A. E. Vladimirov, T. W. Jones, Mon. Not. R. Astron. Soc, **407**: 1773 (2010)
15 D. Caprioli, Journal of Cosmology and Astroparticle Physics, Issue 07, id. 038 (2012)
16 T. Antoni et al, Astrophys. J., **24**: 1 (2005)
17 W. D. Apel et al, Astrophys. J., **31**: 86 (2009)
18 W. D. Apel et al, Astrophys. J., **47**: 54 (2013)
19 D. Caprioli, E. Amato, P. Blasi, Astropart. Phys., **33**: 160 (2010)
20 H. Kang, T. Jones & U. Giedeler, Astrophys. J., **579**: 337 (2002)
21 J. Fang & L. Zhang, Chinese Physics Letters, **25**: 4486 (2008)
22 J. K. Truelove & C. F. McKee, Astrophys. J. Suppl. Ser., **120**: 299 (2009)
23 J. R. Hörandel, N. K. Nikilai & V. T. Alekesi, Astropart. Phys., **27**: 119 (2007)
24 D. Caprioli, E. Amato, P. Blasi, Astropart. Phys., **34**: 447 (2011)
25 B. Bartoli et al, Phys. Rev. D, **85**: 092005 (2012)
26 B. Bartoli et al, CPC, **38**: 045001 (2014)
27 M. Aguilar et al, Phys. Rev. Lett., **114**: 171103 (2015)
28 M. Aguilar et al, Phys. Rev. Lett., **115**: 211101 (2015)
29 O. Adriani et al, Sci. A, **332**: 69 (2011)
30 Y. S. Yoon et al, Astrophys. J., **728**: 122 (2011)
31 M. Amenomori et al, ASR, **47**: 629 (2011)
32 V. S. Ptuskin, V. N. Zirakashvili & E. S. Seo, Astrophys. J., **718**: 31 (2010)
33 A. W. Strong & I. V. Moskalenko, Astrophys. J., **509**: 212 (1998)